## Title
Attenuation of G1 checkpoint function by the non-genotoxic carcinogen phenobarbital.



## Journal
Carcinogenesis, 19(7)

## ISSN
0143-3334

## Authors
Gonzales, AJ
Christensen, JG
Preston, RJ
et al.

## Publication Date
1998-07-01

## DOI
10.1093/carcin/19.7.1173

**Carcinogenesis** vol.19 no.7 pp.1173–1183, 1998

## ACCELERATED PAPER

# Attenuation of $G_1$ checkpoint function by the non-genotoxic carcinogen phenobarbital

**Andrea J.Gonzales[1,2,3], Jamie G.Christensen[4], R.Julian Preston[5], Thomas L.Goldsworthy[5,6], Thea D.Tlsty[7] and Tony R.Fox[5,8]**

[1]Curriculum in Toxicology, University of North Carolina, Chapel Hill, NC 27709, [4]Department of Toxicology, North Carolina State University, Raleigh, NC 27695, [5]Chemical Industry Institute of Toxicology, 6 Davis Drive, PO Box 12137, Research Triangle Park, NC 27709 and [7]Pathology Department, University of California at San Francisco, 513 Parnassus HSW Room 451, San Francisco, California, USA

Present addresses: [2]Cancer Research Department, Parke-Davis, 2800 Plymouth Rd, Ann Arbor, MI 48105, [6]Integrated Laboratory Systems, PO Box 13501, Research Triangle Park, NC 27709 and [8]Glaxo–Wellcome, Inc., TOX-T1128, Five Moore Drive, Research Triangle Park, NC 27709, USA

[3]To whom correspondence should be addressed
Email: Andrea.Gonzales@wl.com

**Non-genotoxic chemical carcinogens are capable of inducing tumors in rodents without interacting with or directly altering the genetic material. Since a preponderance of evidence suggests that cancer results from the accumulation of genetic alterations, the mechanisms by which many non-genotoxic carcinogens induce genotoxic events remain unclear. The present study investigated whether the mitogenic, non-genotoxic carcinogen phenobarbital (PB) could alter cell-cycle checkpoint controls, thereby indirectly leading to the accumulation of genetic damage. Initial studies involved characterizing cell-cycle checkpoint responses to DNA damage in freshly isolated B6C3F1 mouse hepatocytes. These cells responded to bleomycin-induced DNA damage by arresting in $G_1$ and $G_2$. Cell-cycle arrest was coupled with p53 protein induction; however, $p21^{WAF1}$ protein levels remained unchanged. Studies that utilized hepatocytes isolated from C57BL $p53^{-/-}$ mice showed that the DNA damage-induced $G_1$ cell-cycle arrest was dependent on p53 function, but cell-cycle arrest in $G_2$ was not affected by loss of p53. PB was able to delay and attenuate the $G_1$ checkpoint response without altering $G_2$ checkpoint function. A reduction in p53 protein, but not transcript levels, was observed in hepatocytes exposed to PB. Additionally, PB delayed and attenuated p53 protein induction during DNA damage, which suggests that changes in the p53 protein may be contributing to the attenuated $G_1$ checkpoint response caused by PB. Altered $G_1$ checkpoint function represents an epigenetic mechanism by which phenobarbital may prevent the detection and repair of DNA damage and indirectly increase the frequency of genotoxic events above that occurring spontaneously. Abrogation of checkpoint controls may, thus, play an important mechanistic role in mitogenic, non-genotoxic chemical carcinogenesis.**

***Abbreviations:** AT, ataxia telangiectasia; BrdU, bromodeoxyuridine; CDK, cyclin-dependent kinase; DTT, dithiothreitol; HBSS, Hank's balanced salt solution; PB, phenobarbital; PBS, phosphate-buffered saline; PMSF, phenylmethylsulfonyl fluoride; pRb, retinoblastoma protein; RT-PCR, reverse transcriptase polymerase chain reaction; SDS, sodium dodecylsulfate.

## Introduction

Experimental evidence strongly suggests that cancer results from the accumulation of multiple genetic alterations that occur in a limited number of genes: oncogenes and tumor suppressor genes (1). Not surprisingly, chemicals that can induce gene mutations or gross chromosomal aberrations through direct interaction with the DNA commonly exhibit carcinogenic activity (2). What is less obvious is how some carcinogens that do not possess genotoxic properties (non-genotoxicants) are capable of producing the genetic events associated with cancer development.

Mitogenic, non-genotoxic carcinogens induce tumors in rodents without interacting directly with the DNA. These agents are capable of inducing hyperplastic cell proliferation in the absence of necrosis (3), and they also have been shown to inhibit apoptotic cell death (4,5). Genetic alterations are believed to be induced by oxidative stress and by spontaneous errors in DNA replication and repair during continual cell replication (3,6). All of these activities are believed to contribute to the carcinogenic action of these chemicals.

We hypothesize that many mitogenic, non-genotoxic chemicals may exert their carcinogenic effect in part by altering cell-cycle checkpoint controls. Cell-cycle checkpoints function to maintain genomic integrity (7). They act as surveillance systems capable of recognizing genetic alterations or situations that may lead to genetic damage. They also are capable of inducing signals that allow the cell to respond appropriately to DNA damage. If checkpoint function is lost, DNA repair systems may not have time to remove potentially mutagenic or clastogenic DNA lesions before they are fixed during DNA replication and mitosis (8). Loss of checkpoint responses can, therefore, lead to genomic instability (9–11), which plays an integral role in neoplastic transformation (12).

Several genes have been shown to be involved in cell-cycle checkpoint responses to DNA damage. The most extensively studied pathway, the p53-dependent $G_1$ checkpoint response to DNA damage, appears to involve three key genes: *ATM* (mutated in ataxia telangiectasia*) (13,14), *p53* (15,16) and $p21^{WAF1}$ (17,18). The *ATM* gene(s) acts upstream of *p53* and is thought to be involved in p53 protein induction, which occurs immediately after genetic damage (13). p53, in turn, transcriptionally activates a variety of genes including $p21^{WAF1}$ (17). The $p21^{WAF1}$ protein links the DNA damage response pathway to the cell-cycle machinery. $p21^{WAF1}$ associates with $G_1$ cyclin–CDK complexes and can inhibit their kinase activity (18–20). This event leads to the accumulation of hypophosphorylated pRb and prevents the activation of E2F, which is needed for S-phase progression (21).

To determine if mitogenic, non-genotoxic chemicals exert their carcinogenic effect in part by altering cell-cycle checkpoint controls, we investigated whether phenobarbital (PB) could alter checkpoint responses to DNA damage in B6C3F1 mouse hepatocytes. PB is a barbiturate and is also considered to be a mitogenic, non-genotoxic hepatocarcinogen in rodents

(22). This chemical is negative in many short-term genotoxicity assays (22,23); however, male B6C3F1 mice eventually develop liver tumors after chronic exposure (24). Initial studies involving the characterization of checkpoint responses to DNA damage in mouse hepatocytes revealed that these cells arrested in $G_1$ and $G_2$ in response to bleomycin-induced DNA damage. Subsequent experiments found that PB was able to delay and attenuate $G_1$ checkpoint function without affecting the $G_2$ checkpoint response. Hepatocytes exposed to PB exhibited lower steady-state levels of p53 protein, but transcript levels were unaffected. Additionally, PB delayed and attenuated p53 protein induction during DNA damage, which suggests that changes in the p53 protein may be contributing to the attenuated $G_1$ checkpoint response caused by PB. Thus, we believe that abrogation of checkpoint controls may play an important mechanistic role in non-genotoxic hepatocarcinogenesis.

## Materials and methods

*Hepatocyte isolation*

The use of mice was conducted under the National Institutes of Health guidelines for the care and use of laboratory animals and approved by the Institutional Animal Care and Use Committee, Chemical Industry Institute of Toxicology (CIIT). Liver cells were isolated from either B6C3F1 or C57BL male mice, 30 days of age, according to a modified collagenase perfusion procedure described in Kedderis *et al*. (25). Young mice, whose liver cells were still proliferating, were used to ensure that isolated hepatocytes maintained their proliferative capacity throughout the duration of our experiments in culture. B6C3F1 male mice arrived from Charles River (Raleigh, NC) 1 day prior to use. C57BL male mice ($p53^{+/+}$ or $p53^{-/-}$) were obtained from Dr Terry VanDyke at the University of North Carolina at Chapel Hill when needed. Animals were anesthetized with Nembutal (0.02 ml/10 g body wt, i.p.). The peritoneal cavity was then opened, and the vena cave was cannulated using a 20-gauge Angiocath (Deseret Medical Inc., Becton Dickinson, Bedford, MA). The portal vein was cut, and the perfusion was begun *in situ* at 2 ml/min with Hank's balanced salt solution (HBSS; Gibco, Grand Island, NY) containing 0.5 mM EGTA and 10 mM HEPES, pH 7.3 at 37°C. The perfusion was continued for 8 min. The perfusate was then switched to Williams' medium E (Gibco), which contained collagenase (28.8 U/ml; Worthington Biochemical Corp., Freehold, NJ) and HEPES buffer (10 mM), pH 7.3 at 37°C and perfusion was continued for 10 min. The remainder of the procedure followed that described in Kedderis *et al*. (25). Hepatocytes were purified from the liver cell collection by centrifugation at 500 *g* through a Percoll (Sigma, St Louis, MO) solution containing HBSS. Since hepatocytes are much larger and heavier than non-parenchymal cells, this purification procedure easily separates hepatocyte populations from non-parenchymal cells.

*Study design*

For all experiments conducted, freshly isolated B6C3F1 mouse hepatocytes were immediately placed in 100-mm culture dishes at a density of $5\times10^5$ cells per dish and allowed to attach for 14 h. Hepatocytes were cultured in DMEM/F12 medium (Gibco, BRL) that contained 10% fetal calf serum (Hyclone Laboratories, Inc., Logan, UT), ITS™ Premix (Collaborative Biomedical Products, Bedford, MA) and 0.3% nystatin (Gibco, BRL).

Four treatment groups were designed: (i) non-treated hepatocyte controls, (ii) hepatocytes treated with 2 mM PB (Sigma), (iii) hepatocytes treated with 16 μg/ml bleomycin (Sigma) and (iv) hepatocytes pre-treated with 2 mM PB then exposed to 16 μg/ml bleomycin. Hepatocytes exposed to 2 mM PB were treated with PB 14 h after cells were plated. Hepatocytes were exposed to PB for ~23 h. After the 23 h incubation, appropriate cells were exposed to 16 μg/ml bleomycin. (Activity of 16 μg/ml bleomycin ranged from 0.0192 to 0.0272 units of activity per ml.) Samples were collected at various times after bleomycin exposure began for several types of analyses described below. All experiments followed this study design (Figure 1). Time points evaluated after initiation of bleomycin exposure varied among experiments and are noted in the figures and figure legends.

*Cell-cycle analyses*

Cell-cycle analyses were performed on isolated nuclei using a flow cytometric procedure developed and described by White *et al*. (11). Deviations from the protocol included incubating cultured B6C3F1 mouse hepatocytes with 10 μM bromodeoxyuridine (BrdU) for only 3 h prior to fixation and analyzing nuclei preparations with a Becton Dickinson FACS Vantage instrument using Lysis II software.

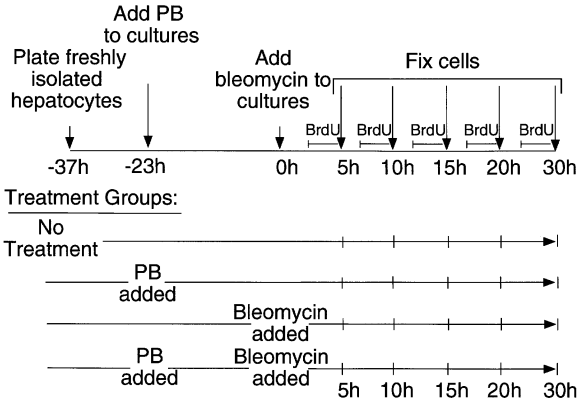


**Fig. 1.** Study design.

To assess $G_1$ checkpoint responses to DNA damage in mouse hepatocytes, we looked for retention of cells in $G_1$ and emptying of cells from early S-phase. Data were plotted as $G_1$/S ratios over time. The percent of cells in $G_1$ and early S-phase could only be determined for diploid populations of hepatocytes and not for tetraploid populations. This limitation occurred because tetraploid $G_1$ populations could not be distinguished from diploid $G_2$ cells, and tetraploid early S-phase cells could not be distinguished from diploid late S-phase cells since their DNA content was the same.

To assess $G_2$ checkpoint responses to DNA damage in mouse hepatocytes, we looked for accumulation of cells in $G_2$ and absence of cells in mitosis. The percent of cells in $G_2$ could only be determined for tetraploid populations of hepatocytes, since diploid $G_2$ cells contained the same amount of DNA as tetraploid $G_1$ cells and, therefore, could not be distinguished from each other.

*Detection of hepatocytes in mitosis*

Cells in mitosis were visualized using cell staining techniques. Specifically, cell culture media were removed from 100-mm plates containing cultured B6C3F1 mouse hepatocytes. Cells were briefly fixed with a mixture of acetic acid and methanol (1:3 v/v). Plates were gently washed with tap water then left to dry. Hepatocytes were stained with 4% Giemsa to visualize cells in mitosis. Two thousand cells were counted per plate, and three plates per treatment group were included.

*Isolation and detection of cellular proteins*

Cellular proteins were isolated and detected using immunoprecipitating and Western blotting techniques. Non-treated and treated hepatocytes in culture were washed three times with cold phosphate-buffered saline (PBS). Hepatocytes were scraped from plates and pelleted. Cell pellets were lysed in an NP-40 lysis buffer [50 mM Tris-base (pH 7.4), 150 mM NaCl, 0.5% NP-40, 50 mM NaF, 1 mM $Na_2VO_3$, 1 mM dithiothreitol (DTT), 1 mM phenylmethylsulfonyl fluoride (PMSF), 10 μg/ml leupeptin, 10 μg/ml aprotinin and 2 μg/ml pepstatin A] for 40 min to release cellular proteins. Lysates were collected and spun at 15 000 *g* for 15 min to remove cellular debris. To isolate p53 protein, 300 μg of cellular lysate were incubated with a mouse monoclonal anti-p53 immunoglobulin (Ig) G antibody (Pab 421; gift from Dr Terry VanDyke) overnight at 4°C. $p21^{WAF1}$ protein was isolated by incubating 300 μg of cellular lysate with a rabbit polyclonal anti-$p21^{WAF1}$ IgG antibody (Santa Cruz) overnight at 4°C. ImmunoPure Immobilized Protein A agarose beads (Pierce Chemical Co., Rockford, IL) were added to immunoprecipitation reactions for 1 h to adsorb the antigen–antibody complexes. Immunoprecipitates were collected and washed four times [50 mM Tris-base (pH 7.4), 150 mM NaCl, 0.5% NP-40, 50 mM NaF, 1 mM $Na_2VO_3$, 1 mM DTT and 1 mM PMSF]. Antigen–antibody complexes were dissociated by resuspending beads in sodium dodecylsulfate (SDS)-sample buffer [2.5% SDS, 25% glycerol, 25 mM Tris-base (pH 8.0) 2.5 mM EDTA, 0.1 M DTT and pyronin Y]. Samples were then boiled at 100°C for 3 min and separated on 17.5% SDS–polyacrylamide gels. Proteins were transferred to a polyvinyl membrane (PVDF; Immobilon-P, Millipore) for Western blotting using a Bio-Rad Trans-Blot Cell. PVDF membranes were blocked for 1 h with 5% non-fat dry milk in PBS containing 0.1% polyoxyethylene-sorbitan monolaurate (Tween 20). After blocking, membranes were washed with PBS–Tween 20 then incubated with primary antibody (1 μg/ml of primary diluted in PBS–Tween) overnight at 4°C. A rabbit polyclonal anti-p53 IgG antibody used for Western blotting was obtained from Vector Laboratories. The same antibody used for immunoprecipitating $p21^{WAF1}$ was also used for Western blotting. Membranes were washed and exposed to an anti-rabbit immunoglobulin coupled to horseradish peroxidase (1:10 000 dilution; Amersham). Specific

proteins were detected using an enhanced chemiluminescence system by Amersham and visualized on ECL-Hyperfilm (Amersham). An image of protein bands was captured using Image I™ software, and bands were quantitated by densitometry using NIH Image software. At least three independent experiments were conducted for all immunoprecipitation reactions coupled with Western blotting.

*Detection of apoptotic hepatocytes*

Mouse hepatocytes were stained with acridine orange (0.25 μg/ml) and ethidium bromide (0.25 μg/ml) to visualize cells undergoing apoptosis. Apoptotic cells, those containing stained pycnotic nuclei, were viewed and counted immediately after staining using fluorescent microscopy. Measurements were obtained from three independent experiments.

*Detection of DNA double strand breaks*

DNA double strand breaks were separated using pulse field gel electrophoresis. Cells were embedded in agarose (0.8% agarose and 10 mM EDTA in PBS, Sigma) and incubated overnight in cell lysis buffer [0.3% mg/ml proteinase K, Boehringer Mannheim, and 1% (w/v) *N*-lauroylsarcosine in 0.5 M EDTA] at 50°C. Agarose plugs were then washed twice in TE-20 buffer (20 mM Tris–HCl, pH 7.4 and 20 mM EDTA). Samples were loaded onto an 0.8% agarose gel and run on a Bio-Rad Chef Mapper electrophoresis cell for 23 h. Pulse time ramped from 20 to 40 min with a voltage gradient of 2 V/cm for 19.5 h followed by a 120° switch angle, pulse time 8–20 s with a voltage gradient of 6 V/cm for 3.5 h. Strand breaks were visualized by staining the gel with ethidium bromide (400 μg/liter). An image was captured using Image I™ software, and strand breaks were quantitated by densitometry using NIH Image software. Strand breaks were measured in samples collected from three independent experiments.

*Competitive reverse transcriptase polymerase chain reaction (RT-PCR)*

p53 mRNA levels were analyzed using competitive RT-PCR. Total RNA was isolated using the RNAzol™ B method (Tel-Test, Inc., Friendswood, TX). Reverse transcription reactions were performed using 1 μg of total RNA and Superscript™II Reverse Transcriptase (Gibco, BRL), following the manufacturer's protocol. An aliquot of 1 μl of the 20 μl cDNA reaction was used as a template to amplify p53 cDNA. Reactions consisted of 50 pmol of each primer (sense: CAAAAAACTTACCAGGGCAAC; antisense: CCACCCGGATAAGATGCTG), PCR buffer (Perkin–Elmer), 200 μM of each dNTP (Gibco, BRL), 8 μCi of [α-$^{32}$P]dCTP (Amersham), 1 pg of internal standard (a portion of the bacterial LacI gene flanked by p53 target sequences recognized by the above primers) and 1.0 U AmpliTaq® DNA Polymerase (Perkin–Elmer). Reactions were heated to 94°C for 2 min before 30 cycles of melting (94°C for 1 min), annealing (60°C for 1 min) and extension (72°C for 45 s) steps were completed. A final incubation at 60°C for 7 min was performed to complete any extensions. The reactions yielded a 295 bp fragment that represented an amplified portion of the *p53* target gene and a 395 bp fragment, which represented the amplified internal LacI standard. Aliquots of 20 μl of the 50 μl reaction mix were separated on a 6% polyacrylamide gel, then the gel was dried. The target gene and internal standard were visualized by exposing the dried gel to a BI phosphor screen (Bio-Rad Laboratories). Ratios of target gene to internal standard were determined using Molecular Analyst Software (Bio-Rad). Measurements were obtained from three independent experiments.

## Results

### *Characterization of checkpoint responses to DNA damage*

To assess the $G_1$ checkpoint response to DNA damage, progression of cells from $G_1$ into S-phase during exposure to bleomycin was monitored in diploid hepatocyte populations using flow cytometric techniques. Progression was evaluated by plotting $G_1$/S ratios over time. Flow cytometric analyses revealed that $G_1$/S ratios increased within 10 h of exposure to bleomycin. These ratios were significantly greater than ratios obtained from non-treated hepatocytes at all time points evaluated, except at 5 h (Figures 2 and 3). The observed increase in $G_1$/S ratios during treatment with bleomycin was caused by retention of cells in $G_1$ and exiting of cells from S-phase.

To assess the $G_2$ checkpoint response to DNA damage, entrance of cells into mitosis was monitored during exposure to bleomycin. Thirty-five mitotic figures were observed (per 2000 cells) in non-treated hepatocytes. The frequency of cells found in mitosis decreased to zero within 5 h after bleomycin treatment began (Table I). Thus, hepatocytes treated with bleomycin arrested in $G_1$ and $G_2$, whereas hepatocytes in S-phase exited.

### *Dependence of checkpoint responses on p53*

Molecular changes associated with bleomycin-induced cell-cycle arrest were also evaluated. In mouse hepatocytes, a 5-fold induction of p53 protein was observed within 5 h of exposure as determined by immunoprecipitating and immunoblotting techniques. At 30 h, p53 levels averaged a 2.5-fold increase relative to non-treated hepatocytes (Figure 4). Interestingly, $p21^{WAF1}$ protein induction was not observed after the addition of bleomycin (Figure 4), nor was there an observed increase in CDK2-associated $p21^{WAF1}$ protein (data not shown).

To further examine the role of p53 in the DNA damage-induced $G_1$ cell-cycle arrest in mouse hepatocytes, cell-cycle progression in the presence or absence of DNA damage was evaluated in hepatocytes isolated from C57BL mice that contained or lacked functional copies of both *p53* genes. Representing data as $G_1$/S ratios allowed for changes in $G_1$ checkpoint responses to be detected even when the predominant cell-cycle arrest occurred in $G_2$. Our reasoning was as follows: When the $G_1$ checkpoint is intact, entry of cells into S-phase ceases, and cells are retained in $G_1$. These cell-cycle changes cause an increase in $G_1$/S ratios over time. If the $G_1$ checkpoint is lost, cells continue to exit from $G_1$ and transit into S-phase at the same rate as non-treated, cycling cells. Thus, $G_1$/S ratios remain similar to non-treated cells, even when the overall percentages of cells in $G_1$ and S-phase are decreasing because of an arrest in $G_2$.

$G_1$/S ratios obtained from C57BL ($p53^{+/+}$) mouse hepatocytes exposed to bleomycin had increased significantly by 10 h of treatment. This effect was similar to that seen in B6C3F1 mouse hepatocytes treated with bleomycin (Figure 5A and D). C57BL hepatocytes that lacked functional *p53* genes did not display a significant increase in $G_1$/S ratios during exposure to bleomycin at any of the time points examined. Instead, ratios remained similar to non-treated, cycling hepatocytes (Figure 5A and D). Thus a functional $G_1$ checkpoint did not exist in hepatocytes lacking *p53*.

The percentage of cells in (diploid and tetraploid) S-phase and (tetraploid) $G_2$/M was also determined in C57BL ($p53^{-/-}$) mouse hepatocytes exposed to bleomycin in order to evaluate the role of p53 in $G_2$ checkpoint responses. In $p53^{-/-}$ mouse hepatocytes, the percent of cells in S-phase was significantly reduced in the present of DNA damage, but not to the extent seen in $p53^{+/+}$ cells (Figure 5B and D). Additionally, accumulation of cells in $G_2$/M was observed in $p53^{-/-}$ mouse hepatocytes exposed to bleomycin (Figure 5C and D). No cells in mitosis could be visualized in $p53^{-/-}$ mouse hepatocytes exposed to bleomycin for 10 h or longer, which suggests that cells were accumulating specifically in $G_2$. Thus, a functional $G_2$ checkpoint appeared to be present in mouse hepatocytes that lacked *p53*.

### *Altered $G_1$ checkpoint response by phenobarbital*

To determine whether the non-genotoxic carcinogen PB could alter checkpoint responses to DNA damage, freshly isolated B6C3F1 mouse hepatocytes were treated with PB ~23 h prior to exposure to bleomycin (see Figure 1 for study design). Results obtained from flow cytometric analyses showed that the $G_1$/S ratios for diploid hepatocytes treated with bleomycin and PB resembled non-treated cells through to 9 h. Beyond

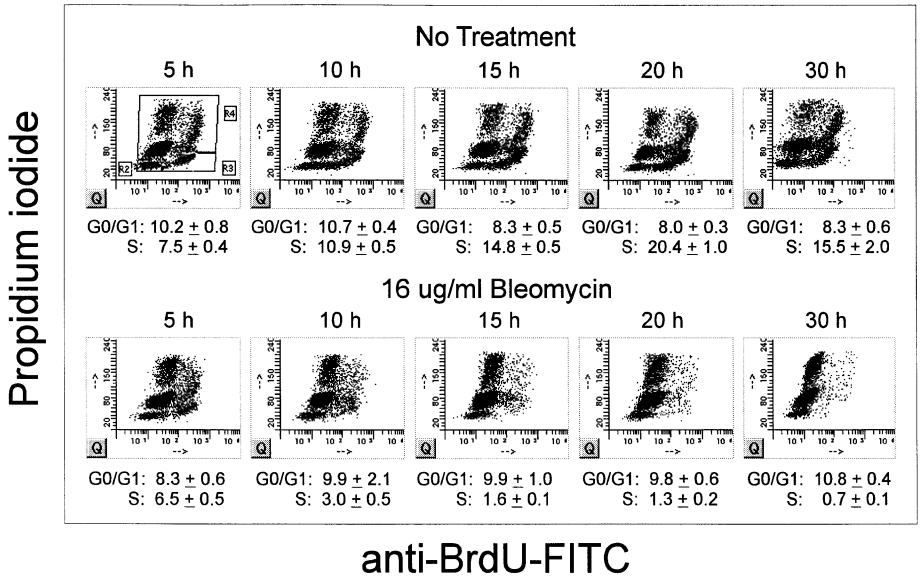


**Fig. 2.** Cell-cycle distribution of mouse hepatocytes. Flow cytometric techniques were used to generate dot plots that depict the distribution of cells throughout the cell cycle in non-treated hepatocytes and hepatocytes exposed to 16 μg/ml bleomycin for 5, 10, 15, 20 and 30 h. Anti-BrdU-FITC (green) fluorescence is plotted on the *x*-axis and represents cells undergoing DNA synthesis. Propidium iodide (red) fluorescence is plotted on the *y*-axis and represents total DNA content. Five thousand events are displayed in each dot plot, and the percent of cells in diploid $G_0/G_1$ and diploid S-phase are shown below each plot as the mean ± 1 SD ($n = 3$). Results were reproduced in three independent experiments involving three separate hepatocyte isolations.

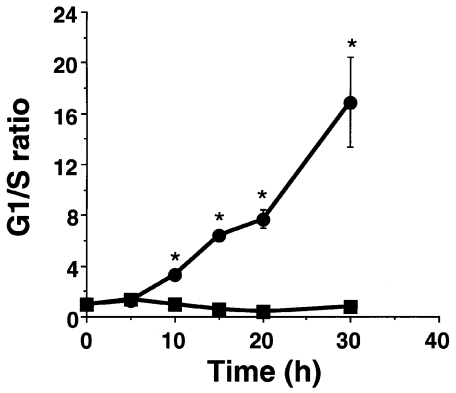


**Fig. 3.** $G_1/S$ ratios were obtained by determining the percentage of cells in diploid $G_1$ (e.g. lower left-hand gate displayed in first dot-plot from Figure 2) and diploid S phases (e.g. lower right-hand gate displayed in first dot-plot from Figure 2). Ratios were plotted over time for non-treated (■) and bleomycin-treated (●) hepatocytes. Plotted values (from a representative experiment) depict means ± 1 SD ($n = 3$). Data were analyzed for each time point using a Student's *t*-test. *Significant difference between non-treated control and 16 μg/ml bleomycin treated hepatocytes ($P < 0.01$). Results were reproduced in three independent experiments involving three separate hepatocyte isolations.

**Table I.** Hepatocytes in mitosis 5 h after the initiation of bleomycin treatment

| Treatment group | Mitotic cells counted (per 2000 cells) |
|---|---|
| Non-treated control | 35.5 ± 5.5 |
| 2 mM PB | 35.3 ± 6.5 |
| 16 μg/ml bleomycin (bleo) | 0 ± 0[a] |
| 2 mM PB + 16 μg/ml bleo | 0 ± 0[a] |

[a]Significantly different from non-treated and PB-treated controls, based on ANOVA and *post hoc* Tukey–Kramer analysis ($P < 0.01$).

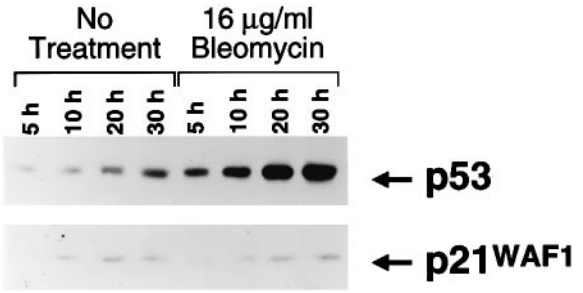


**Fig. 4.** Protein levels of p53 and $p21^{WAF1}$. The p53 and $p21^{WAF1}$ proteins were immunoprecipitated from cellular lysates collected from non-treated mouse hepatocytes and hepatocytes exposed to 16 μg/ml bleomycin for 5 h (lanes 1 and 5, respectively), 10 h (lanes 2 and 6, respectively), 20 h (lanes 3 and 7, respectively) and 30 h (lanes 4 and 8, respectively). Immunoprecipitates were separated by SDS–PAGE and transferred to a polyvinyl membrane for immunoblotting. Results were reproduced in five independent experiments.

the 9 h time point, ratios began to increase but still remained significantly lower than ratios from cells exposed to bleomycin only (Figure 6A). Phenobarbital was able to decrease $G_1/S$ ratios in a concentration-dependent manner (Figure 7) but did not alter the $G_2$ checkpoint response to DNA damage as shown by the lack of cells in mitosis in hepatocytes exposed to PB and bleomycin (Table I).

Other explanations that could account for the lower $G_1/S$ ratios observed in diploid hepatocytes treated with PB plus bleomycin were explored. We observed that hepatocytes pre-treated with PB exhibited a significant decrease in the percentage of cells in diploid $G_1$ after bleomycin treatment when compared with hepatocytes treated only with bleomycin (Figure 6B). Therefore, the possibility existed that PB may have enhanced hepatocyte cell death in the $G_1$ population of cells exposed to bleomycin. Such a change could shift $G_1/S$ ratios to lower values, as seen throughout the time course for this treatment group. To investigate this possibility, cell numbers were compared over time between hepatocytes treated with

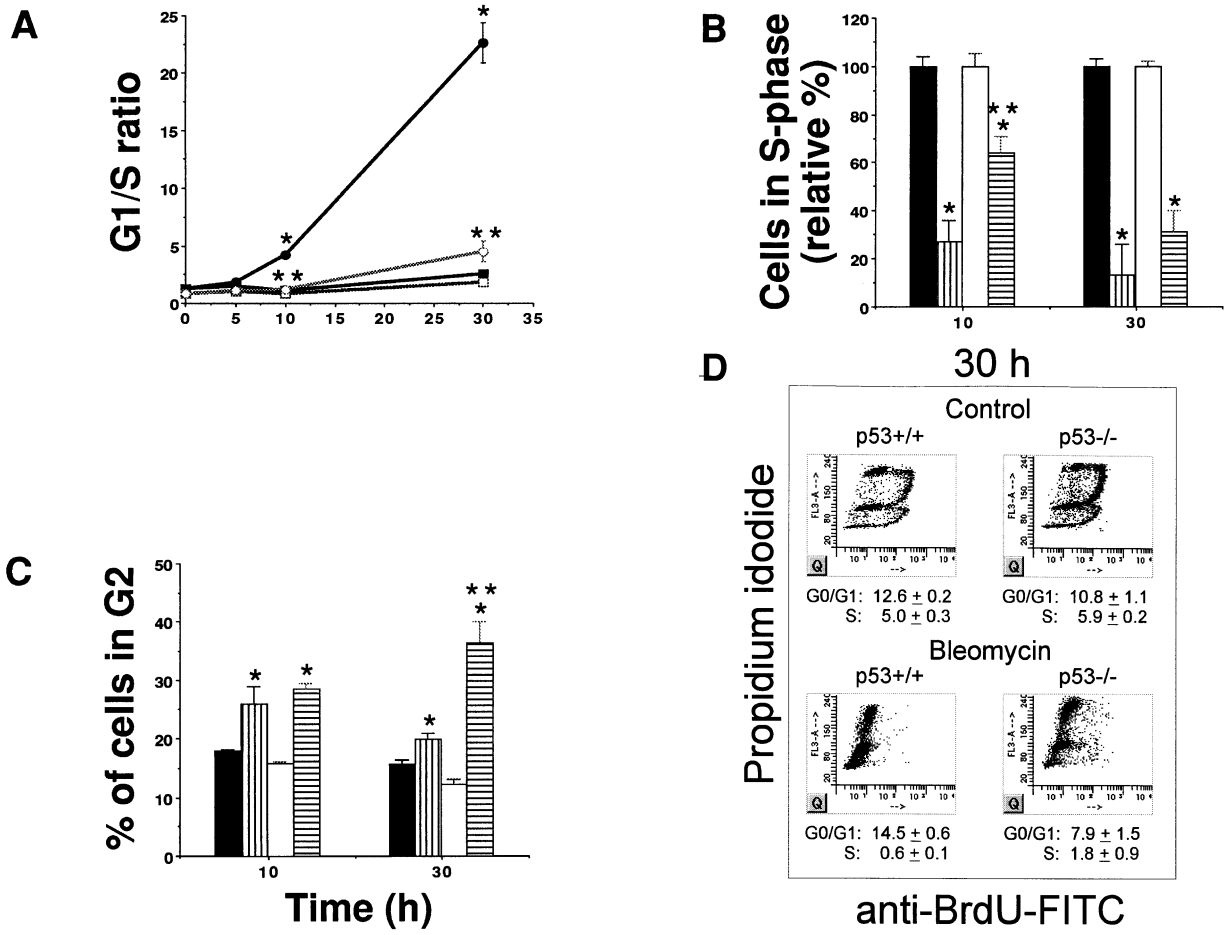


**Fig. 5.** Dependence of the DNA damage-induced $G_1$ checkpoint response on p53 function. Hepatocytes isolated from 30-day-old male C57BL $p53^{+/+}$ and C57BL $p53^{-/-}$ mice were exposed to 16 μg/ml bleomycin for 10 and 30 h and prepared for flow cytometric analysis along with non-treated hepatocytes. (**A**) $G_1$/S ratios were determined for non-treated $p53^{+/+}$ (■) and $p53^{-/-}$ hepatocytes (□) as well as bleomycin-treated $p53^{+/+}$ (●) and $p53^{-/-}$ (○) hepatocytes. Plotted values (from a representative experiment) depict means ± 1 SD ($n = 3$). (**B**) Relative percent of cells in diploid and tetraploid S-phase expressed as the percentage of non-treated control and (**C**) percentage of cells in tetraploid $G_2$/M were determined for non-treated $p53^{+/+}$ (■) and $p53^{-/-}$ hepatocytes (□) as well as bleomycin-treated $p53^{+/+}$ (vertical shaded) and $p53^{-/-}$ (horizontal shaded) hepatocytes. Plotted values (from a representative experiment) depict means ± 1 SD ($n = 3$). An analysis of variance was performed for data presented in all three figures, which was followed by a Tukey–Kramer *post hoc* analysis. *Significant difference from non-treated controls ($P < 0.05$). **Significant difference between bleomycin treated $p53^{+/+}$ and $p53^{-/-}$ hepatocytes ($P < 0.05$). Results were reproduced in two independent experiments involving two separate hepatocyte isolations. (**D**) Flow cytometric analyses of hepatocytes from both $p53^{+/+}$ and $p53^{-/-}$ C57BL male mice non-treated or exposed to 16 μg/ml bleomycin for 30 h are illustrated. Five thousand events are displayed in each dot plot, and the percentage of cells in diploid $G_0/G_1$ and diploid S-phase used to determine $G_1$/S ratios in (A) are listed below each plot. Plotted values represent the mean ± 1 SD ($n = 3$).

PB plus bleomycin and hepatocytes treated with bleomycin only. No significant differences in cell counts were found between the two treatment groups (data not shown). Apoptotic cell death was also measured over the time course for each treatment group. Interestingly, PB appeared to protect against bleomycin-induced apoptosis (Figure 8A and B). Therefore, increased necrotic or apoptotic cell death did not account for the lower proportion of cells in diploid $G_1$ exhibited by hepatocytes treated with PB plus bleomycin.

Since PB appeared to protect cells from bleomycin-induced apoptosis, $G_1$/S ratios obtained from hepatocytes exposed to PB and bleomycin may have been lower because of the preferential protection of S-phase cells from apoptotic cell death. The S-phase fraction of hepatocytes treated with both PB and bleomycin was not significantly greater than the percentage of hepatocytes in S-phase treated only with bleomycin (data not shown). Therefore this possibility did not account for the lower $G_1$/S ratios found in hepatocytes treated with PB and bleomycin.

A third explanation that could account for the lower $G_1$/S ratios exhibited by DNA-damaged cells pre-treated with phenobarbital is that PB may somehow protect cells from genetic damage induced by bleomycin. To address this possibility, DNA double strand breaks were evaluated in cells using pulse-field gel electrophoresis. No significant difference was observed in the amount of double strand breaks present in hepatocytes treated with bleomycin only compared with cells pre-treated with phenobarbital then exposed to bleomycin (Figure 9A and B). Thus, phenobarbital did not appear to protect against bleomycin-induced DNA damage.

*Effect of phenobarbital treatment on p53 protein levels*

The evidence provided so far, strongly suggests that the $G_1$ checkpoint response in diploid hepatocytes was delayed and attenuated by the non-genotoxic carcinogen phenobarbital. Since the mouse hepatocyte $G_1$ checkpoint response appeared to involve p53 (Figure 5), the effects of PB on p53 protein levels were examined. p53 protein was immunoprecipitated

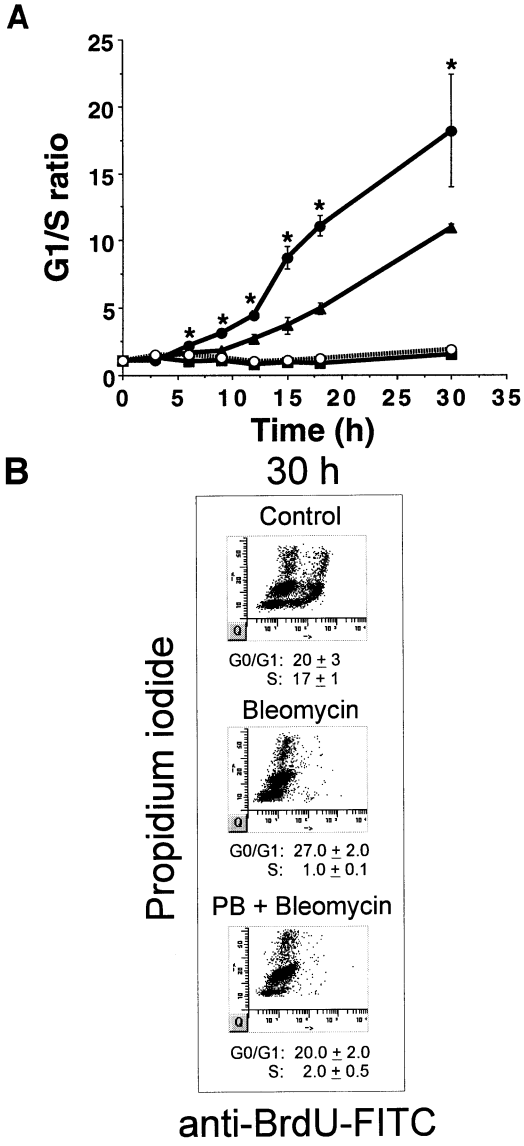


**Fig. 6.** Effect of phenobarbital on $G_1$ checkpoint response in mouse hepatocytes. Cell-cycle progression was assessed at 3, 6, 9, 12, 15, 18 and 30 h after treatment with bleomycin began. (**A**) $G_1$/S ratios for non-treated (■), phenobarbital-treated (○), bleomycin-treated (●) and PB plus bleomycin-treated (▲), hepatocytes were obtained. Plotted values (from a representative experiment) depict means ± 1 SD ($n = 3$). An analysis of variance was performed for data at each time point followed by a Tukey–Kramer *post hoc* analysis. *Significant difference between bleomycin only and PB + bleomycin-treated groups ($P < 0.05$). Results were reproduced in three independent experiments involving three separate hepatocyte isolations. (**B**) Flow cytometric analyses of non-treated hepatocytes and hepatocytes exposed to either 16 μg/ml bleomycin only or 2 mM PB + 16 μg/ml bleomycin for 30 h are illustrated. Five thousand events are displayed in each dot plot, and the percent of cells in diploid $G_0/G_1$ and diploid S-phase are listed below each plot and represent the mean ± 1 SD ($n = 3$).

from cellular lysates collected from non-treated hepatocytes and hepatocytes treated with phenobarbital. PB-treated hepatocytes exhibited, on average, a 30% reduction in steady-state levels of p53 protein relative to non-treated hepatocytes (Figure 10). Furthermore, p53 protein induction due to bleomycin exposure was delayed and attenuated in hepatocytes pre-treated with PB (Figure 11). Specifically, p53 protein induction was not observed until the 20 h time point, and peak levels of p53 protein in hepatocytes treated with PB and bleomycin were 60% lower than those observed in hepatocytes treated only with bleomycin. Interestingly, p53 message levels remained unaltered in PB-treated hepatocytes where p53 protein levels were lower relative to the non-treated controls (Figure 12).

*Effect of PB treatment on cell-cycle progression in $p53^{-/-}$ mouse hepatocytes*

The ability of PB to delay and attenuate $G_1$ checkpoint responses to DNA damage correlated with its ability to delay and attenuate induction of p53 protein in response to DNA damage. To more directly investigate the role of p53 in the attenuation of $G_1$ checkpoint responses by PB, cell-cycle progression was evaluated in C57BL $p53^{-/-}$ mouse hepatocytes exposed to PB and/or bleomycin. $G_1$/S ratios obtained from $p53^{-/-}$ hepatocytes exposed to either bleomycin or PB plus bleomycin did not differ from each other or from the non-treated $p53^{-/-}$ hepatocytes (Figure 13A). Thus, comparison of $G_1$/S ratios, which depict effects on only the (diploid) $G_1$ checkpoint response, did not provide additional information, since the $G_1$ checkpoint was dependent on p53.

We also evaluated the effects of PB on cell-cycle progression by comparing the percent of cells in (diploid and tetraploid) S-phase during bleomycin exposure, which is influenced by $G_1$ and $G_2$ checkpoint responses, and by comparing the percentage of cells in (tetraploid) $G_2$/M. In $p53^{-/-}$ mouse hepatocytes, the percent decrease in S-phase cells in response to bleomycin exposure was not altered by PB (Figure 13B). Accumulation of $p53^{-/-}$ cells in $G_2$ because of bleomycin treatment was also not affected by PB (Figure 13C). Therefore cell-cycle distribution of hepatocytes exposed to bleomycin was not altered by PB in cells lacking p53.

## Discussion

The present study was performed to determine whether the mitogenic, non-genotoxic carcinogen PB could alter cell-cycle checkpoint responses to DNA damage. We found that PB was able to delay and attenuate the $G_1$ checkpoint response in diploid hepatocytes without affecting the ability of cells to arrest in $G_2$. Hepatocytes treated with PB contained lower steady-state levels of the p53 protein without exhibiting changes in p53 message levels. In addition, PB was able to delay and attenuate induction of p53 protein in response to DNA damage. These observations suggest that the ability of PB to alter $G_1$ checkpoint responses was mediated, in part, through *p53*. We believe these findings provide evidence for a novel epigenetic mechanism by which mitogenic, non-genotoxic chemicals may exert their carcinogenic effect.

Since checkpoint responses to DNA damage have not been previously described in primary cultures of mouse hepatocytes, a considerable amount of time was spent on characterizing these responses to determine whether they were similar to those observed in human cell systems. Primary cultures of B6C3F1 mouse hepatocytes reacted to DNA damage by arresting in $G_1$ and $G_2$. Induction of p53 protein was also observed within 5 h of exposure to bleomcyin. C57BL mouse hepatocytes that lacked functional copies of both *p53* genes did not arrest in $G_1$, but instead continued to transit into S-phase similar to non-treated hepatocytes. These studies reveal that the $G_1$ checkpoint response in mouse hepatocytes was dependent on *p53*, consistent with signaling molecules identified as participating in checkpoint responses in many human cell systems (11,13,16,18).

Interestingly a significant decrease in S-phase cells was observed in the $p53^{-/-}$ mouse hepatocytes exposed to bleo-

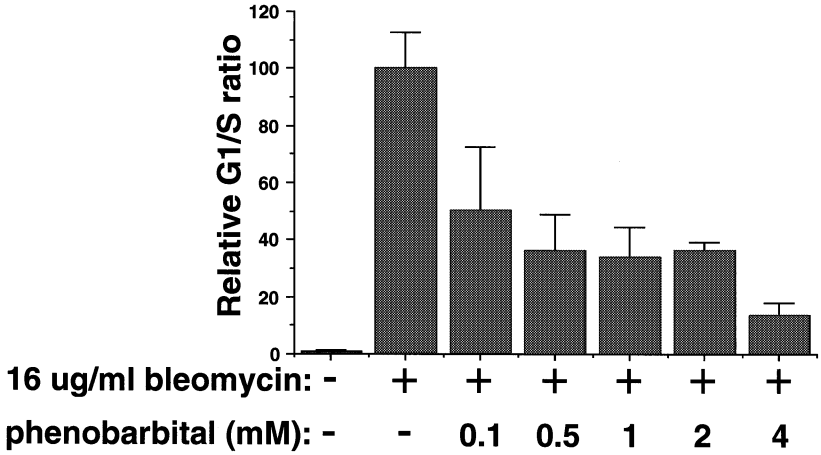


**Fig. 7.** Concentration-dependent effect of phenobarbital on $G_1$/S ratios. Hepatocytes were exposed to varying concentrations of phenobarbital (100 μM to 4 mM). At 23 h after the addition of phenobarbital, bleomycin was added to the medium (16 μg/ml). Hepatocytes were collected 30 h after bleomycin exposure began and were prepared for flow cytometric analysis to determine $G_1$/S ratios. $G_1$/S ratios were expressed as the percentage of bleomycin-only-treated control. Relative values represent means ± 1 SD ($n$ = 3).

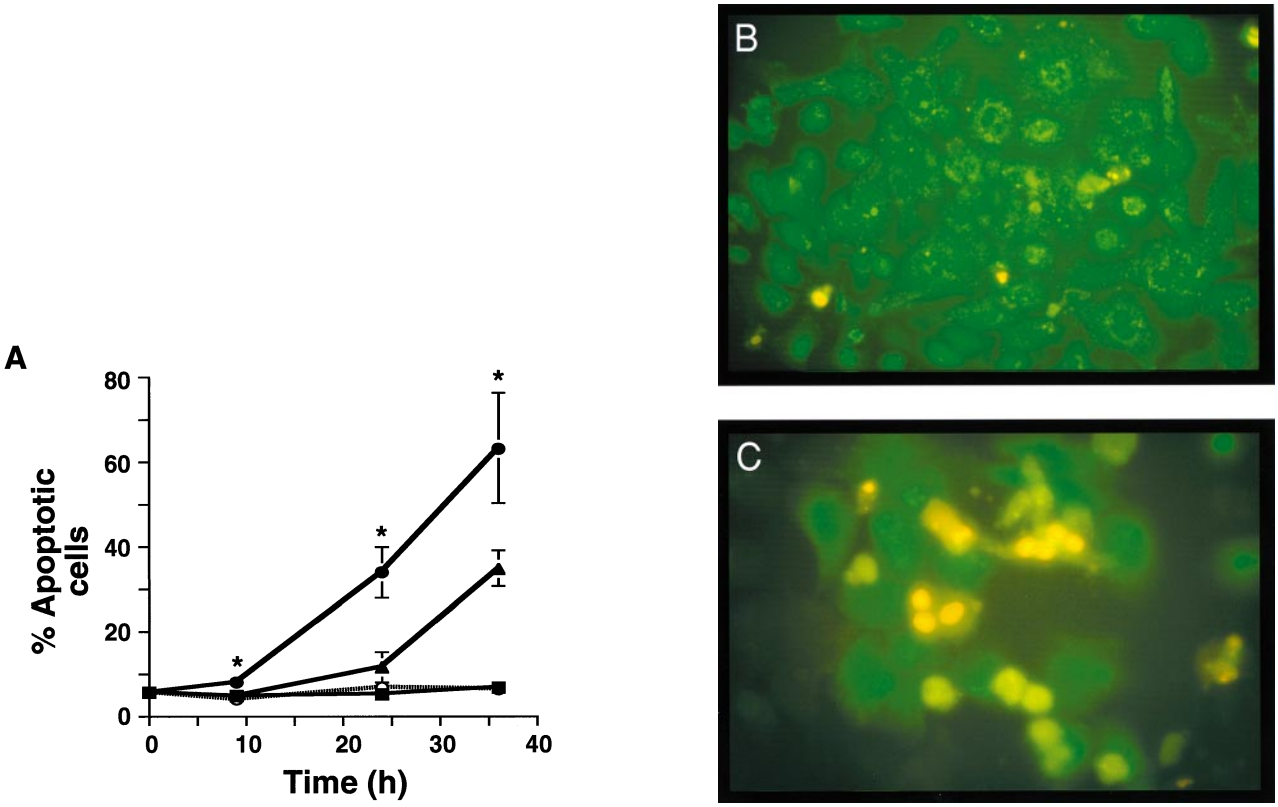


**Fig. 8.** Apoptotic cell death of mouse hepatocytes. (**A**) Non-treated (■), phenobarbital-treated (○), bleomycin-treated (●) and PB plus bleomycin-treated (▲), mouse hepatocytes were stained with acridine orange (0.25 μg/ml) and ethidium bromide (0.25 μg/ml) at 8, 24 and 36 h of exposure to bleomycin to detect apoptotic cells. Cells were viewed and scored using fluorescent microscopy. Results were reproduced in three independent experiments involving three separate hepatocyte isolations. Values represent means ± 1 SD ($n$ = 3). Fluorescent photomicrographs of (**B**) non-treated hepatocytes and (**C**) hepatocytes exposed to 16 μg/ml bleomycin for 36 h are presented. Cells exhibiting an orange fluorescent, pycnotic nucleus are apoptotic, and cells staining a dull yellow with no visibly distinct nucleus represent necrotic cells.

mycin, which suggests that other checkpoint responses remained intact. A decrease in the percentage of cells in S-phase is dependent on both $G_1$ and $G_2$ checkpoint responses. The $G_1$ checkpoint retains cells in $G_1$ and prevents entry into S-phase. The $G_2$ checkpoint halts cells in $G_2$ and prevents them from cycling through M-phase and back into $G_1$. We believe that the ability of *p53*$^{-/-}$ cells to exhibit a significant reduction in S-phase in response to DNA damage may be due to the ability of the $G_2$ checkpoint to respond even in the absence of p53. This idea is further supported by our observations that *p53*$^{-/-}$ mouse hepatocytes accumulated in the $G_2$ phase of the cell cycle during bleomycin exposure, halting cell-cycle progression. The role of p53 in $G_2$ checkpoint function remains controversial, but our studies suggest that the mouse hepatocyte $G_2$ checkpoint response to DNA damage is independent of p53 function. (The reduction of S-phase in

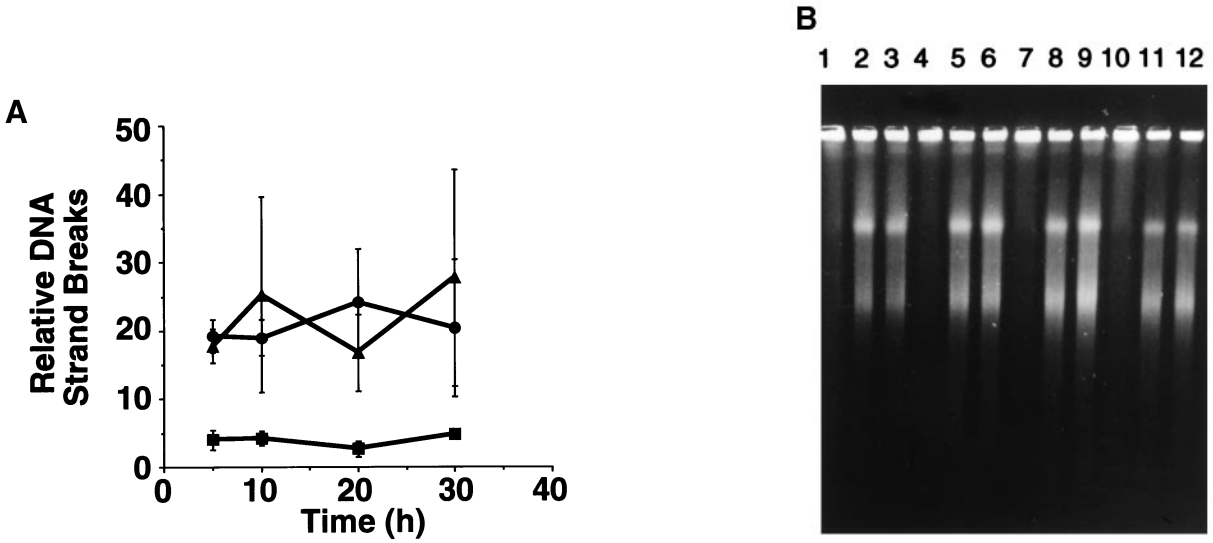


**Fig. 9.** DNA double strand breaks. (**A**) DNA strand breaks were measured in non-treated (■), bleomycin-treated (●) and PB plus bleomycin-treated (▲) mouse hepatocytes using pulse field gel electrophoresis. Breaks were evaluated for each treatment group at 5, 10, 20 and 30 h after bleomycin exposure was initiated. Results were reproduced in three independent experiments involving three separate hepatocyte isolations. Values represent means ± 1 SD ($n$ = 3). (**B**) Strand breaks were visualized by staining agarose gels with ethidium bromide (400 μg/liter). Lanes 2, 5, 8 and 11 depict strand breaks from hepatocytes exposed to 16 μg/ml bleomycin for 5, 10 , 20 and 30 h, respectively. Lanes 3, 6, 9 and 12 show strand breaks from hepatocytes exposed to 2 mM PB plus 16 μg/ml bleomycin for 5, 10, 20 and 30 h, respectively. Lanes 1, 4, 7 and 10 depict strand breaks from the time-matched non-treated hepatocytes.

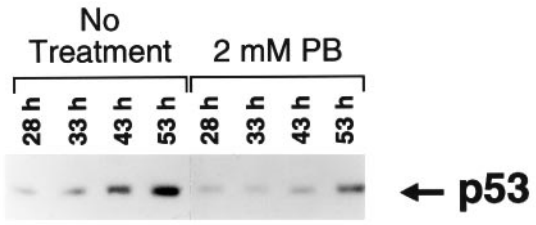


**Fig. 10.** Lower p53 protein levels in hepatocytes treated with phenobarbital. p53 protein was immunoprecipitated from cellular lysates collected from non-treated hepatocytes and hepatocytes treated with 2 mM phenobarbital for 28 h (lanes 1 and 5, respectively), 33 h (lanes 2 and 6, respectively), 43 h (lanes 3 and 7, respectively) and 53 h (lanes 4 and 8, respectively). Immunoprecipitates were separated by SDS–PAGE, proteins were transferred to a polyvinyl membrane, and p53 protein was detected by immunoblotting. Results were reproduced in four independent experiments involving four separate hepatocyte isolations.

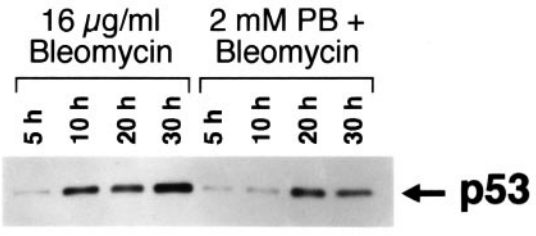


**Fig. 11.** Delayed p53 protein induction in response to DNA damage in hepatocytes exposed to phenobarbital. p53 protein was immunoprecipitated from cellular lysates collected from hepatocytes exposed to 16 μg/ml bleomycin and cells treated with 2 mM PB plus 16 μg/ml bleomycin for 5 h (lanes 1 and 5, respectively), 10 h (lanes 2 and 6, respectively), 20 h (lanes 3 and 7, respectively) and 30 h (lanes 4 and 8, respectively). Since cells exposed to PB + bleomycin were incubated with PB for 23 h prior to the addition of bleomycin, exposure of cells to bleomycin for 5, 10, 20 and 30 h meant the PB plus bleomycin treated cells were exposed to PB for 28, 33, 43 and 53 h, respectively. Therefore Figures 10 and 11 can be compared.

*p53*$^{-/-}$ mouse hepatocytes exposed to DNA damage did not reach the extent seen in treated *p53*$^{+/+}$ cells, probably because of the loss of $G_1$ checkpoint function in *p53*$^{-/-}$ cells, which would allow cells from $G_1$ to transit into S-phase, even in the presence of DNA damage.)

Although p53 appeared to play a role in $G_1$ checkpoint function, p21$^{WAF1}$ protein induction was not observed in response to DNA damage in mouse hepatocytes. *p21*$^{WAF1}$ is one of several genes identified as playing a role in the p53-dependent $G_1$ checkpoint response to DNA damage in human cells (17,18). Immediately after genetic damage, p53 protein levels dramatically increase (13). p53 in turn transcriptionally activates a variety of genes, including *p21*$^{WAF1}$ (17). The p21$^{WAF1}$ protein can associate with $G_1$ cyclin–CDK complexes and inhibit their kinase activity (18–20). This event leads to the accumulation of hypophosphorylated pRb and prevents the activation of E2F and progression into S-phase (21).

Even though p21$^{WAF1}$ protein induction was not observed in hepatocytes exposed to bleomycin, we believe that p53 was transcriptionally active. We were able to detect the induction of other *p53* target genes, such as *bax* (27; and data not shown). The possibility still exists, however, that lack of p21$^{WAF1}$ protein induction in B6C3F1 mouse hepatocytes during bleomycin exposure may be an artifact of our model system. Nevertheless, hepatocytes were capable of arresting in $G_1$ in the presence of DNA damage despite the lack of induction of p21$^{WAF1}$ protein.

Finding a lack of p21$^{WAF1}$ protein induction after the addition of bleomycin raises the possibility that other molecules may be involved in p53-mediated checkpoint responses to DNA damage. Studies involving mouse epithelial cells within the intestinal crypts or mouse embryo fibroblasts demonstrated that the $G_1$ checkpoint response was either independent or only partially dependent on p21$^{WAF1}$ function, respectively (28–30). Other studies have found that p21$^{WAF1}$ protein levels do not always increase with induction of p53 protein and cell-cycle arrest (31). Our studies provide another example where

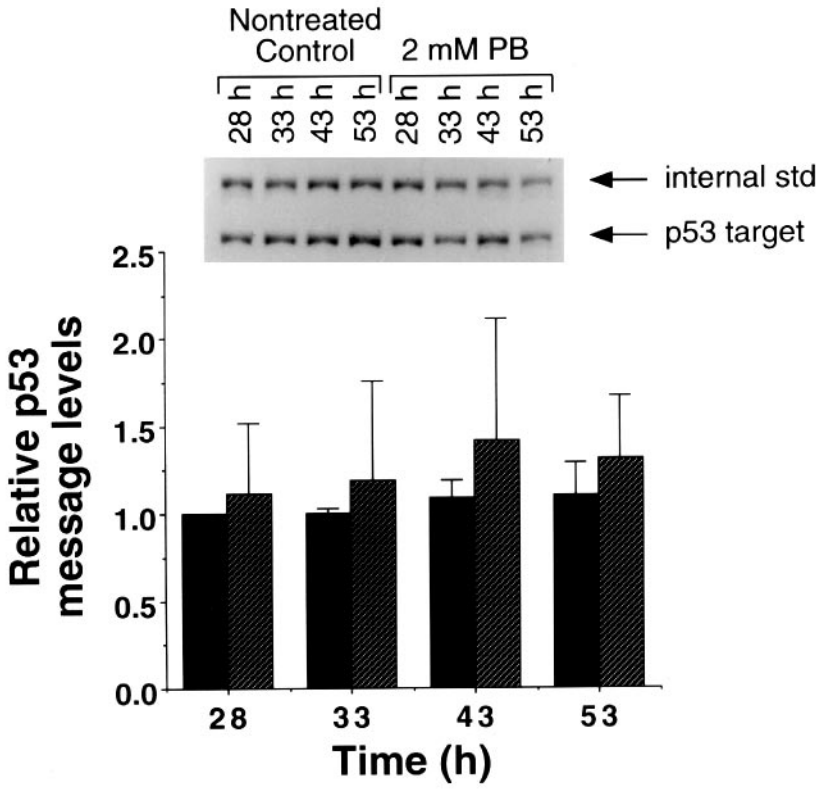


**Fig. 12.** p53 Message levels in hepatocytes exposed to phenobarbital. Total RNA was isolated from non-treated hepatocytes (■) and hepatocytes exposed to 2 mM phenobarbital (shaded) for 28, 33, 43 and 53 h. Message levels of p53 were quantitated using the technique of competitive RT-PCR. This technique yielded a 295 bp fragment, which represented an amplified portion of the *p53* target gene, and a 395 bp fragment, which represented the amplified internal LacI standard. Results were reproduced in three independent experiments involving three separate hepatocyte isolations and RNA isolations. Values represent means ± 1 SD ($n = 3$).

$p21^{WAF1}$ protein induction may not occur during cell-cycle checkpoint responses.

Other molecules that may be involved in mouse hepatocyte cell-cycle checkpoints may include *GADD45*, a p53-dependent, DNA damage-inducible gene capable of inhibiting cell-cycle progression when overexpressed (32) or other CDK inhibitory proteins. Alternatively other mechanisms, such as tyrosine-phosphorylation of CDK4, could be involved (33). Regardless, the identification of these checkpoint genes and/or pathways will allow for new targets to be investigated in mitogenic, non-genotoxic carcinogenesis.

After characterization of checkpoint responses to DNA damage in mouse hepatocytes was complete, we evaluated the ability of phenobarbital to abrogate these checkpoint responses. Lower $G_1$/S ratios in cells treated with PB and bleomycin as compared with cells treated with only bleomycin suggested that PB delayed and attenuated the $G_1$ checkpoint response to DNA damage. Lower $G_1$/S ratios were caused by a significant decrease in the percentage of cells in $G_1$, which suggests that PB-treated cells continued to enter S-phase even in the presence of DNA damage. Abrogation of checkpoint controls has been shown to have deleterious effects on a cell. Failure to arrest in $G_1$ in the presence of DNA damage could prevent the repair of damaged DNA and, in turn, lead to the replication of damaged genetic material. If mutations were to occur in proto-oncogenes or tumor suppressor genes, such alterations could provide a growth advantage and additional genomic instability, allow for the survival and clonal expansion of pre-cancerous cells and the eventual progression to a complete neoplastic phenotype.

Several changes in p53 were observed in cells exposed to PB. Hepatocytes treated with PB contained lower steady-state levels of the p53 protein, and PB treatment was able to delay and attenuate induction of p53 protein in response to DNA damage. Since PB treatment did not alter steady-state levels of p53 mRNA, the effects of PB on p53 appeared to occur at the level of translation or post-translationally. *p53* gene mutations are rare in chemically induced mouse liver tumors (34–38) even though it is the most frequently mutated gene in human cancers (39). Thus, the possibility exists that epigenetic changes in p53 protein may occur more frequently in chemically-induced hepatocarcinogenesis than alterations in the *p53* gene.

Changes in p53 protein described above during PB treatment suggest that abrogation of $G_1$ checkpoint function by PB was mediated through effects on p53. If this were true, then one would predict that PB could not alter checkpoint responses, which function independent of p53. In our study, the $G_2$ checkpoint response to DNA damage in mouse hepatocytes appeared to be independent of p53 function since hepatocytes isolated from $p53^{-/-}$ mice were capable of exiting from S-phase and arresting in $G_2$ when treated with bleomycin. Interestingly, the $G_2$ checkpoint response to DNA damage was not altered by PB in B6C3F1 ($p53^{+/+}$) or C57BL ($p53^{-/-}$) mouse hepatocytes, which supports our hypothesis.

Since abrogation of $G_1$ checkpoint function by PB

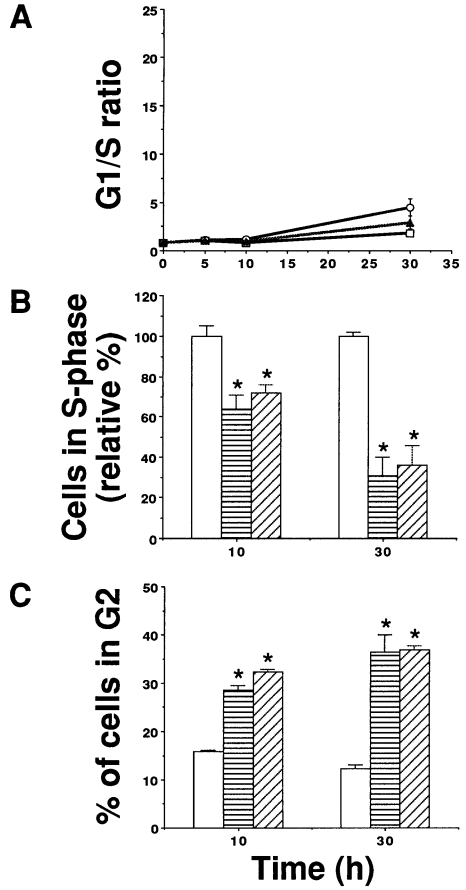


**Fig. 13.** Effect of PB treatment on cell-cycle progression in $p53^{-/-}$ mouse hepatocytes. Cell-cycle progression was assessed in C57BL $p53^{+/+}$ and $p53^{-/-}$ hepatocytes at 5, 10 and 30 h after treatment with bleomycin began, using flow cytometric techniques. (**A**) $G_1$/S ratios were determined for non-treated $p53^{-/-}$ hepatocytes (□), $p53^{-/-}$ hepatocytes exposed to 16 μg/ml bleomycin (○) and $p53^{-/-}$ hepatocytes exposed to 2 mM PB plus 16 μg/ml bleomycin (▲). Plotted values (from a representative experiment) depict means ± 1 SD ($n = 3$). (**B**) Relative percent of cells in diploid and tetraploid S-phase expressed as the percent of non-treated control, and (**C**) percent of cells in tetraploid $G_2$/M were determined for non-treated $p53^{-/-}$ hepatocytes (□), $p53^{-/-}$ hepatocytes exposed to 16 μg/ml bleomycin (horizontal shading) and $p53^{-/-}$ hepatocytes exposed to 2 mM PB plus 16 μg/ml bleomycin (diagonal shading) were obtained. Plotted values (from a representative experiment) depict means ± 1 SD ($n = 3$). An analysis of variance was performed for data presented in all three figures, which was followed by a Tukey–Kramer post hoc analysis. Results were reproduced in two independent experiments that involved two separate hepatocyte isolations. *Significant difference between non-treated controls and hepatocytes exposed to 16 μg/ml bleomycin ($P < 0.05$).

appeared to be mediated through effects on the p53 protein, the possibility exists that other p53-dependent functions, such as DNA repair or apoptosis, may have been altered by PB in addition to $G_1$ checkpoint responses. Attenuation of these processes could significantly accelerate the cancer process by not only preventing the detection and repair of DNA damage, but also by preventing the elimination of altered cells from the population. We did observe a delayed and attenuated apoptotic response to DNA damage in hepatocytes exposed to PB. These observations were consistent with *in vivo* findings that showed the ability of PB to inhibit apoptosis in the rodent liver (34).

In summary, the present study is the first to demonstrate that the mitogenic, non-genotoxic chemical carcinogen, phenobarbital, can alter a biochemical pathway involved in maintaining genomic integrity (i.e. checkpoint controls). Phenobarbital has traditionally been viewed as an agent that provides a preferential growth stimulus to pre-cancerous and cancerous cells. Thus, many biochemical pathways studied as potential targets for these agents are apoptotic pathways and growth factor pathways involved in cell proliferation. The ability of phenobarbital to alter $G_1$ checkpoint responses to DNA damage represents a novel epigenetic mechanism through which mitogenic, non-genotoxic carcinogens may enhance genotoxic events and genomic instability, key events in the cancer process. A mechanistic understanding of non-genotoxic carcinogenesis will clearly aid in the interpretation of animal study data that are commonly used in human cancer risk assessments. Identification of a biological response (i.e. checkpoint function) targeted by these agents also provides a means to investigate dose–response relationships, potential threshold responses, and similarities or differences in responses among species, including humans.

## Acknowledgements

The authors would like to thank Drs Byron Butterworth, Russel Cattley, Chris Corton, Bill Kaufmann, Phil Ableson and Barbara Kuyper for their critical review of the manuscript. We would also like to thank Drs David Kaufman, William Kaufmann and Terry VanDyke for scientific contributions made to this research project. $p53^{-/-}$ mice along with the mouse monoclonal anti-p53 antibody were generously provided by Dr Terry VanDyke. A.J.Gonzales was supported by a National Research Council Ford Foundation Pre-doctoral Fellowship.

## References

1. Weinberg,R.A. (1994) Oncogenes, antioncogenes, and the molecular bases of multistep carcinogenesis. *Cancer Res.*, **49**, 3713–3723.
2. Shelby,M.D. and Zieger,E. (1990) Activity of human carcinogens in the salmonella and rodent bone-marrow cytogenetics tests. *Mutat. Res.*, **234**, 257–261.
3. Butterworth,B.E., Popp,J.A., Conolly,R.B. and Goldsworthy,T.L. (1992) Chemically induced cell proliferation in carcinogenesis. In Vainio,H., Magee,P.N., McGregor,D.B. and McMichael,A.J. (eds) *Mechanisms of Carcinogenesis in Risk Identification*. Scientific Publications, Lyon, France, pp. 279–305.
4. Marsman,D.S. and Barret,J.C. (1994) Apoptosis and chemical carcinogenesis. *Risk Anal.*, **14**, 321–326.
5. Schulte-Hermann,R., Bursch,W., Grasl-Kraupp,B., Torok,L., Ellinger,A. and Mullauer,L. (1995) Role of active cell death (apoptosis) in multi-stage carcinogenesis. *Toxicol. Lett.*, **82/83**, 143–148.
6. Butterworth,B.E., Conolly,R.B. and Morgan,K.T. (1995) A strategy for establishing mode of action of chemical carcinogens as a guide for approaches to risk assessments. *Cancer Lett.*, **93**, 129–146.
7. Hartwell,L.H. and Weinhert,T.A. (1989) Checkpoints: Controls that ensure the order of cell cycle events. *Science*, **246**, 629–633.
8. Kaufmann,W.K. and Wilson,S.R. (1994) $G_1$ arrest during cell cycle dependent clastogenesis in UV-irradiated human fibroblasts. *Mutat. Res.*, **314**, 67–76.
9. Livingstone,L.R., White,A., Sprouse,J., Livanos,E., Jacks,T. and Tlsty,T.D. (1992) Altered cell cycle arrest and gene amplification potential accompany loss of wild-type *p53*. *Cell*, **70**, 923–935.
10. Yin,Y., Tainsky,M.A., Bischoff,F.Z., Strong,L.C. and Wahl,G.M. (1992) Wild-type *p53* restores cell cycle control and inhibits gene amplification in cells with mutant *p53* alleles. *Cell*, **70**, 937–948.
11. White,A.E., Livanos,E.M. and Tlsty,T.D. (1994) Differential disruption of genomic integrity and cell cycle regulation in normal human fibroblasts by the HPV oncoproteins. *Genes Dev.*, **8**, 666–677.
12. Hartwell,L. (1992) Defects in a cell cycle checkpoint may be responsible for the genomic instability of cancer cells. *Cell*, **71**, 543–546.
13. Kastan,M.B., Zhan,Q., El-Deiry,W.S., Carrier,F., Jacks,T., Walsh,W.V., Plunkett,B.S., Vogelstein,B. and Fornace,A.J. Jr (1992) A mammalian cell cycle checkpoint pathway utilizing *p53* and *GADD45* is defective in ataxia-telangiectasia. *Cell*, **71**, 587–597.
14. Savitsky,K., Bar-Shira,A., Gilad,S. *et al.* (1995) A single ataxia

telangiectasia gene with a product similar to PI-3 kinase. *Science*, **268**, 1749–1753.
15. Kastan,M.B., Onyekwere,O., Sidransky,D., Vogelstein,B. and Craig,R.W. (1991) Participation of p53 protein in the cellular response to DNA damage. *Cancer Res.*, **51**, 6304–6311.
16. Kuerbitz,S.J., Plunkett,B.S., Walsh,W.V. and Kastan,M.B. (1992) Wild-type *p53* is a cell cycle checkpoint determinant following irradiation. *Proc. Natl Acad. Sci USA*, **89**, 7491–7495.
17. El-Deiry,W.S., Harper,J.W., O'Connor,P.M. *et al.* (1994) WAF1/CIP1 is induced in *p53*-mediated $G_1$ arrest and apoptosis. *Cancer Res.*, **54**, 1169–1174.
18. Dulic,V., Kaufmann,W.K., Wilson,S., Tlsty,T.D., Lees,E., Harper,J.W., Elledge,S.J. and Reed,S.I. (1994) *p53*-dependent inhibition of cyclin-dependent kinase activity in human fibroblasts during radiation-induced $G_1$ arrest. *Cell*, **76**, 1013–1023.
19. Xiong,Y., Hannon,G.J., Zhang,H., Casso,D., Kobayashi,R. and Beach,D. (1993) p21 is a universal inhibitor of cyclin kinases. *Nature*, **366**, 701–707.
20. Harper,J.W., Adami,G.R., Wei,N., Keyomarsi,K. and Elledge,S.J. (1993) The p21 cdk-interaction protein cip1 is a potent inhibitor of $G_1$ cyclin-dependent kinases. *Cell*, **75**, 805–816.
21. Sherr,C. (1994) $G_1$ phase progression: cycling on cue. *Cell*, **79**, 551–555.
22. ICPEMC (1984) Report of ICPEMC Task Group 5 on the differentiation between genotoxic and non-genotoxic carcinogens. *Mutat. Res.*, **133**, 1–49.
23. Albertini,S. and Gocke,E. (1992) Phenobarbital: Does the positive result in TA1535 indicate genotoxic properties? *Environ. Mol. Mutat.*, **19**, 161–166.
24. Becker,F.F. (1982) Morphological classification of mouse liver tumors based on biological characteristics. *Cancer Res.*, **42**, 3918–3923.
25. Kedderis,G.L., Argenbright,L.S. and Miwa,G.T. (1988) Studies with nitrogen-containing steroids and freshly isolated rat hepatocytes: role of cytochrome P-450 in detoxication. *Toxicol. Appl. Pharmacol.*, **93**, 403–412.
26. Miyashita,T. and Reed,J.C. (1995) Tumor suppressor *p53* is a direct transcriptional activator of the human *bax* gene. *Cell*, **80**, 293–299.
27. Christensen,J.G., Gonzales,A.J. and Goldsworthy,T.L. (1997) Regulation of apoptosis in mouse hepatocytes and alterations by hepatic tumor promoters. *Toxicologist*, **36**, 246.
28. Brugarolas,J., Chandrasekaran,C., Gordon,J.I., Beach,D., Jacks,T. and Hannon,G.J. (1995) Radiation-induced cell cycle arrest compromised by *p21* deficiency. *Nature*, **377**, 552–557.
29. Deng,C., Zhang,P., Harper,J.W., Elledge,S.J. and Leder,P. (1995) Mice lacking $p21^{CIP1/WAF1}$ undergo normal development, but are defective in $G_1$ checkpoint control. *Cell*, **82**, 675–684.
30. Yuan,Z.-M., Huang,Y., Whang,Y., Sawyers,C., Weichselbaum,R., Kharbanda,S. and Kufe,D. (1996) Role for c-Abl tyrosine kinase in growth arrest response to DNA damage. *Nature*, **382**, 272–274.
31. Hirano,Y., Yamato,K. and Tsuchida,N. (1995) A temperature sensitive mutant of the human p53, Val38, arrests rat cell growth without induced expression of *cip1/waf1/sdi* after temperature shift-down. *Oncogene*, **10**, 1879–1885.
32. Smith,M.L., Chen,I.-T., Zhan,Q., Bae,I., Chen,C.-Y., Gilmer,T.M., Kastan,M.B., O'Connor,P.M. and FornaceA.J. Jr (1994) Interaction of the *p53*-regulated protein Gadd45 with proliferating cell nuclear antigen. *Science*, **266**, 1376–1380.
33. Terada,Y., Tatsuka,M., Jinno,S. and Okayama,H. (1995) Requirement for tyrosine phosphorylation of Cdk4 in $G_1$ arrest induced by ultraviolet irradiation. *Nature*, **376**, 358–362.
34. Goodrow,T.L., Storer,R.D., Leander,K.R., Prahalada,S.R., van Zwieten,M.J. and Bradley,M.O. (1992) Murine *p53* intron sequences 5–8 and their use in polymerase chain reaction/direct sequencing analysis of *p53* mutations in CD-1 mouse liver and lung tumors. *Mol. Carcinogenesis*, **5**, 9–15.
35. Kress,S., Konig,J., Schweizer,J., Lohrke,H., Bauer-Hofmann,R. and Schwarz,M. (1992) *p53* mutations are absent from carcinogen-induced mouse liver tumors but occur in cell lines established from these tumors. *Mol. Carcinogenesis*, **6**, 148–158.
36. Hegi,M.E., Soderkvist,P., Foley,J.F., Shoonhoven,R., Swenberg,J.A., Kari,F., Maronpot,R., Anderson,M.W. and Wiseman,R.W. (1993) Characterization of *p53* mutations in methylene chloride-induced lung tumors from B6C3F1 mice. *Carcinogenesis*, **14**, 803–810.
37. Rumsby,P.C., Davies,M.J. and Evans,J.G. (1994) Screening for *p53* mutations in C3H/He mouse liver tumors derived spontaneously or induced with diethylnitrosamine or phenobarbitone. *Mol. Carcinogenesis*, **9**, 71–75.
38. Calvert,R.J., Tashiro,Y., Buzard,G.S., Diwan,B.Z. and Weghorst,C.M. (1995) Lack of *p53* point mutations in chemically induced mouse hepatoblastomas: an end-stage, highly malignant hepatocellular tumor. *Cancer Lett.*, **95**, 175–180.
39. Hollstein,M., Sidransky,D., Vogelstein,B. and Harris,C.C. (1991) *p53* mutations in human cancers. *Science*, **253**, 49–53.
40. Schulte-Hermann,R., Timmermann-Trosiener,I., Barthel,G. and Bursch,W. (1990) DNA synthesis, apoptosis, and phenotypic expression as determinants of growth of altered foci in rat liver during phenobarbital promotion. *Cancer Res.*, **50**, 5127–5135.

*Received on October 1, 1997; revised on March 31, 1998; accepted on April 8, 1998*